

# Forming Stages of Polycrystalline TiN Films Depending on the Nitrogen Concentration in Mixed Gas

Anna L. Kameneva

State Educational Institution of the Higher Vocational Education, Perm State Technical University, Perm, Russia  
Email: annkam789@mail.ru

Received October 6<sup>th</sup>, 2010; revised December 7<sup>th</sup>, 2010; accepted December 13<sup>th</sup>, 2010.

## ABSTRACT

*The influence of nitrogen concentration in mixed gas on temperature conditions, structure and phase composition of the TiN film deposited by arc spraying has been investigated. By electron microscopic investigations and X-ray diffraction phase analysis was recognized forming stages and structuring process of the film with main cubic phase (111) TiN. It was discovered that forming stages and process of structuring of ion-plasma TiN films are affected by both film temperature and its rate of heating.*

**Keywords:** Polycrystalline TiN Film, Arc Spraying, Temperature Conditions, Forming Stages, Structure and Phase Modification

## 1. Introduction

The stabilization and interpretation of properties of ion-plasma polycrystalline films is a fairly complicated problem because of a great variety of factors which influence their characteristics [1-5]. The solution of this problem is impossible without studying the laws that govern the processes of the formation of polycrystalline films depending on technological parameters, as well as without studying phase composition, the structural and morphological features of the relief of the surfaces of the films and its properties [6-19].

The aim of this work is to examine the influence of nitrogen concentration in mixed gas on the temperature conditions, pattern and formation stages, structure formation processes, prevailing orientation direction, phase composition and mechanical properties of TiN films during electric-arc evaporation.

## 2. Methods of the Substrates Preparation, Forming and Investigation of Structure and Conditions of TiN Film

### 2.1. Methods of the Preparation of Substrates and Formation of TiN Film

TiN films were produced using industrial HHB-6,6-И4 unit by means of one electric-arc evaporator with BT1-00

titanium cathode at various nitrogen concentration in mixed gas. To increase the adhesive strength of TiN film on the surface of the test samples Ti underlayer was applied after its ion cleaning-heating.

### 2.2. The Method of Substrate and TiN Film Temperature Control

Temperature of test pieces surface as well as the film temperature after each 10 minutes of the film deposition have been measured by infrared contactless pyrometer after both ionic cleaning and sublayer applying, a whole duration of the precipitation process was 30 minutes.

### 2.3. Methods of Studying the Structure, Phase Composition and Conditions of TiN Film

Morphological traits of the formed films have been investigated by bitmapped electron microscope BS 300 with prefix for microanalysis EDAX Genesis 2000. X-ray diffraction phase analysis of TiN film was carried out using X-ray diffractometer DRON-4 in Cu K $\alpha$  radiation. Microhardness of the composition has been measured by microhardness tester PMT-3 with indenter load of 0.5 N after the film precipitation process.

## 3. Simulation Results and Discussion

The process conditions of the substrate preparing carried

out before the film deposition—ionic-bombardment cleaning and sublayer Ti applying—are given in **Table 1**, and **Table 2** lists the process conditions for the arc spraying, and microhardness of composition TiN film- substrate (hereinafter named as composition microhardness).

### 3.1. Results of the X-Ray Diffractometer Phase Analysis of the TiN Polycrystalline Film

Results of X-ray diffractometer phase analysis of the TiN films deposited by arc spraying with 50% nitrogen concentration and higher are given in **Figure 1**, **Table 3** and **Table 4**. The TiN film consisting of main cubic phase with (111) direction of preferred lattice orientation and auxiliary hexagonal phase of  $\text{TiN}_{0.3}$  is forming on the substrate independently on nitrogen concentration.

The TiN film with maximum microhardness produced at optimal temperature and process parameters of spraying (film heating rate of 14.2 K/min and nitrogen con-

centration in gas mix of 90%) has the following structure characteristics: maximum volume fraction of the cubic phase TiN (111) equal to 99.2%, and minimum the one of hexagonal phase  $\text{TiN}_{0.3}$  (101) equal to 0.8%; minimum deviation of cleavage spacing from table value; maximum peak width of the TiN (111) phase, and minimum the one of  $\text{TiN}_{0.3}$  (101) regardless of heterogeneous inside stresses in the film appearing as a result of various direction of peak coordinate departures of TiN (111) to less angles and the one of  $\text{TiN}_{0.3}$  (101) to most angles.

For the first time it was discovered that decreasing of nitrogen concentration less than 70% leads to increasing of hexagonal phase  $\text{TiN}_{0.3}$  volume fraction in the film: equal parts of argon and nitrogen result in forming disordered two-phase film with maximum deviation of the cleavage spacing from table value and with less value of composition microhardness.

**Table 1. Process conditions of the ionic-bombardment cleaning and sublayer Ti applying.**

Process	U, V	Substrate—plasma source distance, mm	T, min	P, Pa	$I_{\text{focusing coil}}$ , A	$I_{\text{stabilizing coil}}$ , A	$I_{\text{arc}}$ , A	V, rpm	Gas	Final substrate temperature, K
Ionic cleaning	high600	270	5	0.01	1.50	2.50	80	2.5	Ar	651
Sublayer applying	bias200	270	3	1.0	1.50	2.50	80	2.5	Ar	Ar

**Table 2. Process conditions of the TiN film applying by arc spraying.**

Experiment No.	$\text{N}_2$ concentration, %	$L$ , mm	P, Pa	$I_{\text{arc}}$ , A	$U_{\text{bias}}$ , V	$T_{\text{film}}$ , K			$V_{\text{film heat}}$ , K/min	$H_{\mu}$ , GPa
						Process durability, min				
						10	20	30		
1	50					625	640	670	12.3	16.0
2	70	270	1.0	80	200	625	650	680	12.5	21.0
2	90					645	670	725	14.5	27.1

**Table 3. Phase composition and structural characteristics of the TiN films produced by arc spraying:  $V$  is phase inclusion volume fraction,  $d_{\text{TiN}}/d_{\text{TiN}_{\text{table}}}$  is cleavage spacing,  $I_{\text{TiN}}/I_{\text{TiN}_{0.3}}$  is intensity ratio of all reflexes of cubic TiN phase and hexagonal  $\text{TiN}_{0.3}$  the one,  $\max I_{111\text{TiN}}/I_{\Sigma}$  and  $\max I_{101\text{TiN}_{0.3}}/I_{\Sigma}$  are ratios of maximum reflex intensities (111) or (101) to total intensity of all TiN phase reflexes, and  $\beta_0$  is breadth of X-ray diffraction line.**

Experiment No.	$\text{N}_2$ concentration, %	$V$ , %		$d_{\text{TiN}}$	$d_{\text{TiN}_{0.3}}$	$I_{\text{TiN}}$	$I_{\Sigma}$	$\frac{\max I_{111\text{TiN}}}{I_{\Sigma}}$	$\frac{\max I_{101\text{TiN}_{0.3}}}{I_{\Sigma}}$	$\frac{\max I_{\text{TiN}}}{\max I_{\text{TiN}_{0.3}}}$	$\frac{\beta_{111}^0}{\beta_{101}^0}$
		TiN	$\text{TiN}_{0.3}$	$d_{\text{TiN}_{\text{table}}}$ , nm	$d_{\text{TiN}_{0.3\text{table}}}$ , nm	$I_{\text{TiN}_{0.3}}$					
1	50	85.5	14.5	$\frac{0.2458}{0.2450}$	$\frac{0.2257}{0.2268}$	1.87	255	0.65	0.35	1.59	$\frac{1.70}{0.67}$
2	70	98.9	1.1	$\frac{0.2465}{0.2450}$	$\frac{0.2262}{0.2268}$	19.10	100.5	0.81	0.01	54.0	$\frac{2.5}{0.57}$
3	90	99.2	0.8	$\frac{0.2465}{0.2450}$	$\frac{0.2265}{0.2268}$	20.20	106.0	0.76	0.02	32.4	$\frac{3.3}{0.55}$

**Table 4. Positions of the diffraction peaks.**

Film	Phase	Lattice type	Grain orientation	$2\theta_{\text{table}}$ , grad	2 $\theta$ , grad		
					Nitrogen concentration, %		
					50	70	90
TiN	TiN	Volume-centred cubic	<111>	36.8048	36.55	36.45	36.45
	$\text{TiN}_{0.3}$	Hexagonal	<101>	39.7086	39.95	39.85	39.80

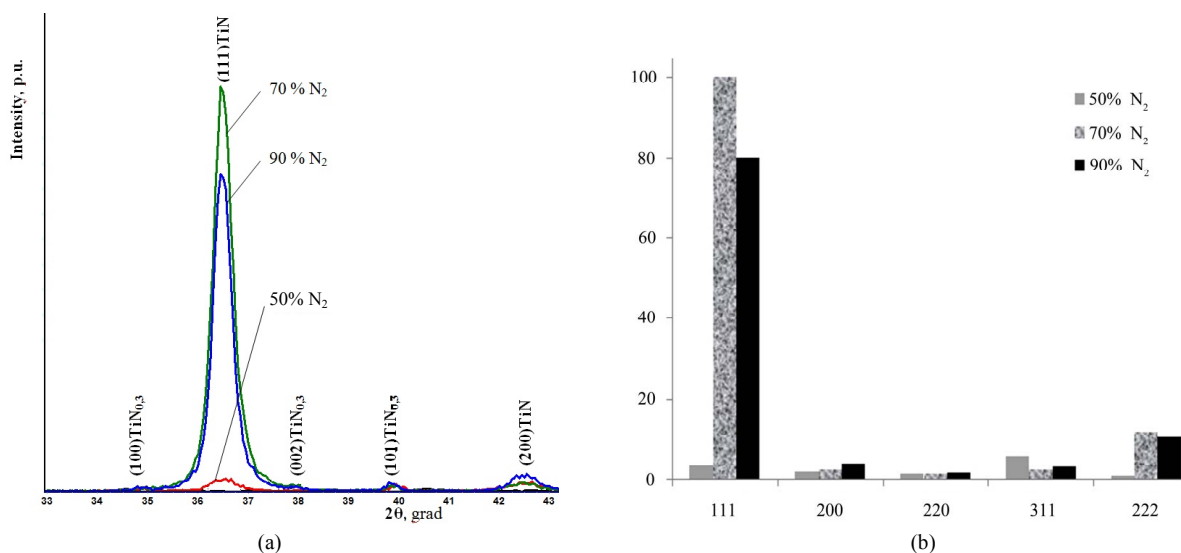


**Figure 1. (a) Comparative band of diffractogram fragments for TiN film pieces produced by arc spraying at various nitrogen concentrations in mixed gas. (b) Comparative diagram of diffraction peaks of the cubic phase TiN reduced to 100% of maximum peak over the range 25...80.**

### 3.2. Results of the Electron Microscopic Investigations of the Polycrystalline TiN Film

Surface morphologies of all produced TiN films have been investigated in order to find a reason of the change of mechanical properties.

Based on morphological investigation at low magnification it was discovered that TiN films formed by arc spraying at various nitrogen concentrations have various roughness (**Figure 2**). Based on investigations of film surface morphology, it was deduced that TiN film forming stages are identical in case of main cubic phase in spite of various volume part ration of phases in the film:

- Globular stage, when there is no directivity of border regions in space. Spherical globules are forming with minimum substrate contact surface (**Figure 3(a)**) in conditions of low temperatures up to 625 K and low substrate wetting. Notwithstanding that decrease of argon concentration in gas mix reduces both ion density and ion mobility, increase in nitrogen concentration boosts film heating rate and initiates van der Waals forces to appear which facilitate the substrate wetting and forming of appanate globular structures with contacting area equal to globule diameter (**Figures 3(b,c)**). Globules having minimum height and diameter are forming at nitrogen concentration of 90% in gas mix.

- Stage of transit of the globular structure to grain substructure. 3D formations are forming on the film surface in direction perpendicular to substrate surface (**Figure 4**). Increasing of film temperature due to its heating rate increase, and increasing of rate of plasma

chemical reaction due to nitrogen concentration increase both together facilitate to a grain substructure ordering (**Figure 4(c)**). The 3D formations with ordered grain substructure correspond to films formed at nitrogen concentration of 90% (**Figure 4(c)**).

- Stage of integration of the 3D formations having grain substructure. Increasing of film forming durability leads to integration of the formations having grain substructure into microsystems of various configurations: single 3D formations and appanate islands with grain substructure (**Figure 5(a)**) at minimum film heating rate  $V_{\text{heat}} = 12.3$  K/min, integration of the 3D formations having grain substructure and initially ordering of their surfaces (**Figure 5(b)**) at  $V_{\text{heat}} = 12.5$  K/min and maximum nitrogen concentration of 90%, integration of the 3D formations having grain substructure to islands with pseudoplain  $\{100\}$  on their surface (**Figure 5(c)**) at  $V_{\text{heat}}$  up to 14.2 K/min and film temperature up to 725 K.

- Stage of nucleation of polycrystalline constituent of the film with main cubic (111) TiN phase (**Figure 6**). It carries in temperature rating of 650 to 670 K at film heating rate of 12.5 to 14.2 K/min. Maximum temperature and film heating rate both facilitate to multiple increasing of seeds number and reducing of crystal grain diameter. Polycrystalline structures in form of seed crystallites with pseudoplain  $\{100\}$ , unidirectional to substrate and equispaced on its surface, germ in process of film deposition at nitrogen concentration of 90% in mixed gas (**Figure 6(c)**).

- Stage of island forming of the polycrystalline film. Stage of nucleation of polycrystalline constituent of film only in conditions of further temperature increasing to

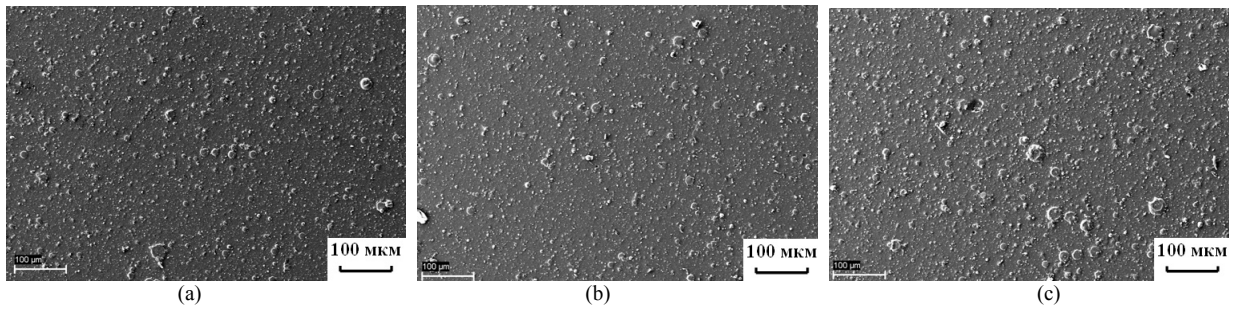


Figure 2. Photomicrographs of TiN films formed by arc spraying at various nitrogen concentration in mixed gas: (a) 50%; (b) 70%; (c) 90%.

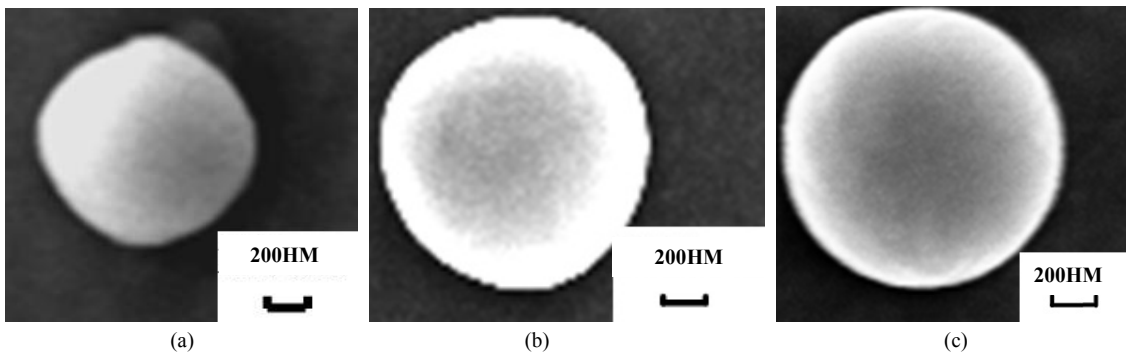


Figure 3. Photomicrographs of the TiN film on globular stage: (a)  $\text{\O} 1.0 \mu\text{m}$  at 50%; (b)  $\text{\O} 1.3 \mu\text{m}$  at 70%; (c)  $\text{\O} 1.2 \mu\text{m}$  at 90%.

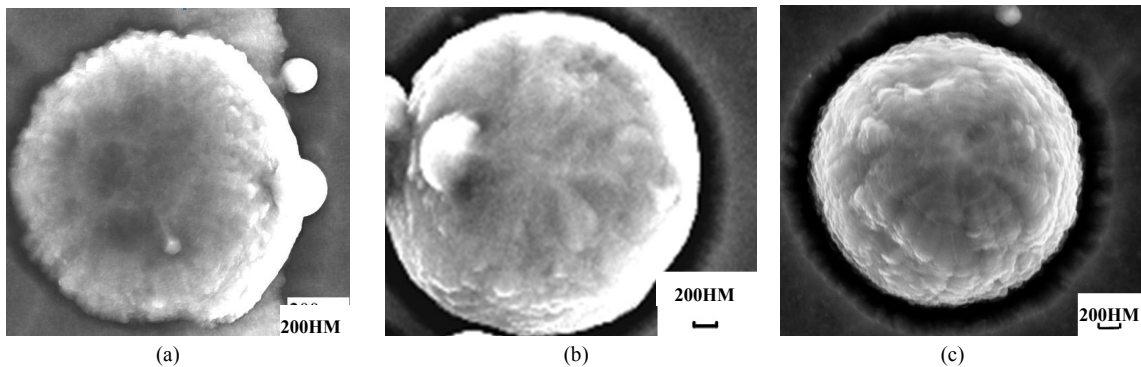


Figure 4. Photomicrographs of the TiN film on the stage of forming of 3D formations with grain substructure: (a)  $\text{\O} 3.0 \mu\text{m}$  at 50%; (b)  $\text{\O} 3.0 \mu\text{m}$  at 70%; (c)  $\text{\O} 720 \text{nm}$  to  $2.5 \mu\text{m}$  at 90%.

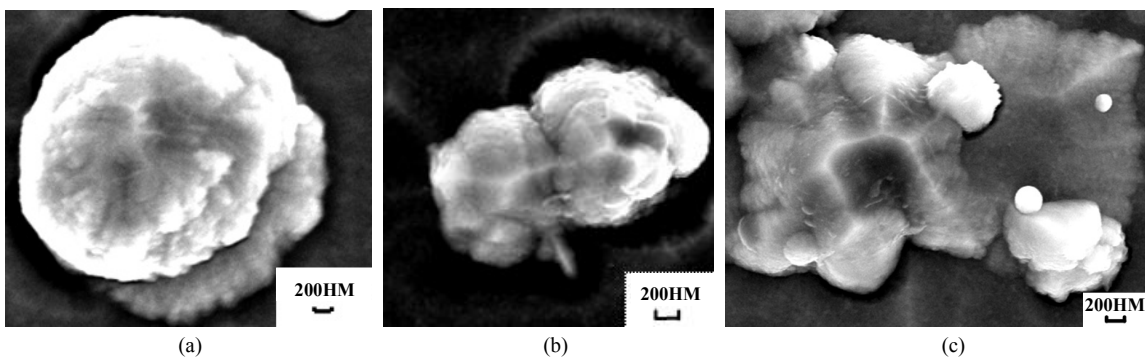
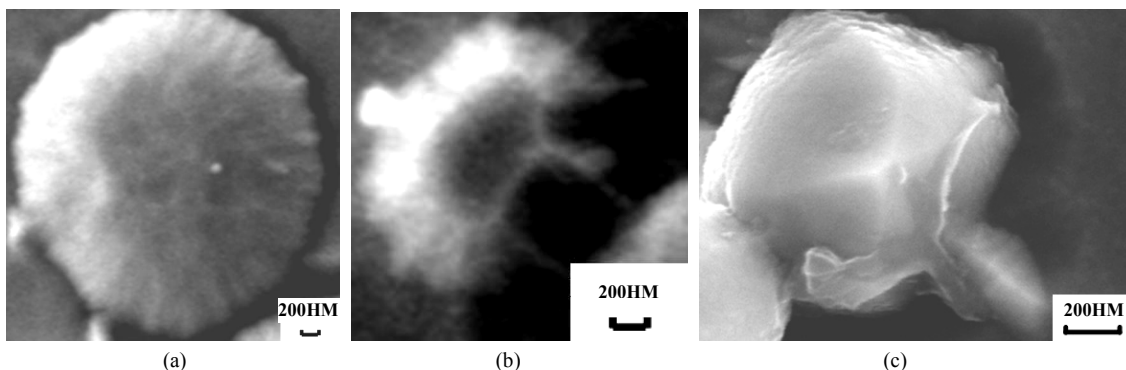


Figure 5. Photomicrographs of the TiN films on stage of integration of 3D formations having grain substructure into microsystems: (a) 3D formations  $\text{\O} 3.3 \mu\text{m}$  at 50% of nitrogen; (b) Integrations with dimension  $L = 2.5 \mu\text{m}$  consisting of globules  $\text{\O} 1.0 \mu\text{m}$  and  $\text{\O} 1.5 \mu\text{m}$  at 70%; (c) Integrations with dimension  $L = 5.0 \mu\text{m}$  consisting of 3D formations with diameter of  $\text{\O} 3.0 \mu\text{m}$  and  $\text{\O} 2.0 \mu\text{m}$  at 90%.



**Figure 6.** Photomicrographs of the TiN film on stage of nucleation in form of: (a) Initial polycrystalline formations in form of frustums with bases of  $1.4 \times 4.0 \mu\text{m}$  at 50% of nitrogen; (b) Seed crystallite in form of frustums with bases of  $0.4 \times 0.9 \mu\text{m}$  and  $1.3 \mu\text{m}$  at 70%; (c) Seed crystallite,  $\text{Ø} 1.2 \mu\text{m}$ , with pseudoplains  $\{100\}$  at 90%.

670... 725 K with heating rate not less than 12.3 K/min goes to stage of forming of 2D polycrystalline formations in form of islands on surface of the film (Figures 7(a-f)). Film temperature increase related to increasing of nitrogen concentration and film deposition duration leads at once to increasing of 2D island diameter and decreasing of both island height and seed crystallite diameter. Maximum increasing of the film temperature and its heating rate up to optimal values of 725 K and 14.2 K/min respectively (90% of nitrogen) facilitates to

multiple increasing of islands number. It will be observed a repetitive forming of 3D formations with grain substructure on surface of polycrystalline islands only at 50% and 70% nitrogen concentration (Figures 7(b,c)).

- Stage of continuous film forming. An electron microscope investigation of the film surface morphology has shown that continuous film formed at surface heating up to 680 K has the cellular structure (Figures 8(a,c)), and at surface heating up to 725 K it has nanodispersed grain the one (Figures 8(e,f)) due to film structure stabilization.

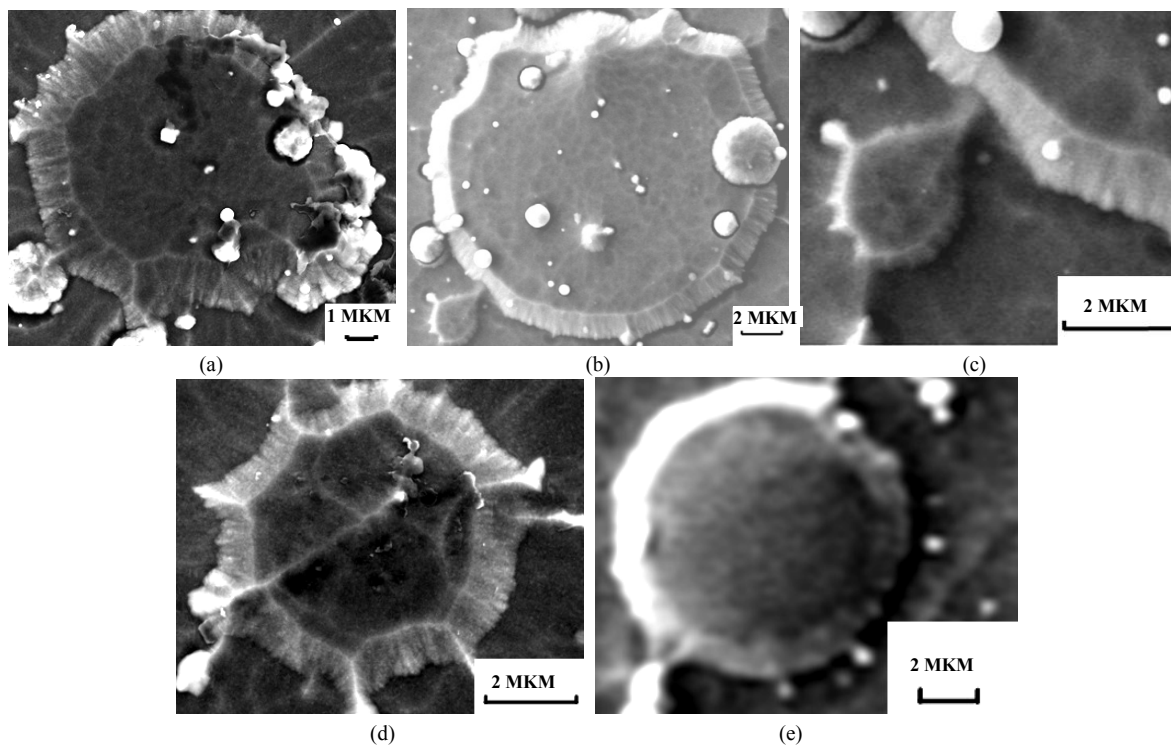


**Figure 7.** Photomicrographs of the TiN film in stage of forming of polycrystalline 2D islands with following dimensions: (a)  $\text{Ø} 10.0 \mu\text{m}$  and height  $H = 1.5 \mu\text{m}$  at 50% of nitrogen; (b) Max  $\text{Ø} 16.5 \mu\text{m}$  and  $H = 1.0 \mu\text{m}$ , min  $\text{Ø} 2.5 \mu\text{m}$  and  $H = 0.3 \mu\text{m}$ , limit distance between islands for their integration is 700 nm (forced fragment right), all at 70%; (c)  $\text{Ø} 4.0 \mu\text{m}$  and  $H = 1.0 \mu\text{m}$ ; and (d)  $\text{Ø} 9.0 \mu\text{m}$  and  $H = 1.0 \mu\text{m}$ , both latter at 90% of nitrogen.

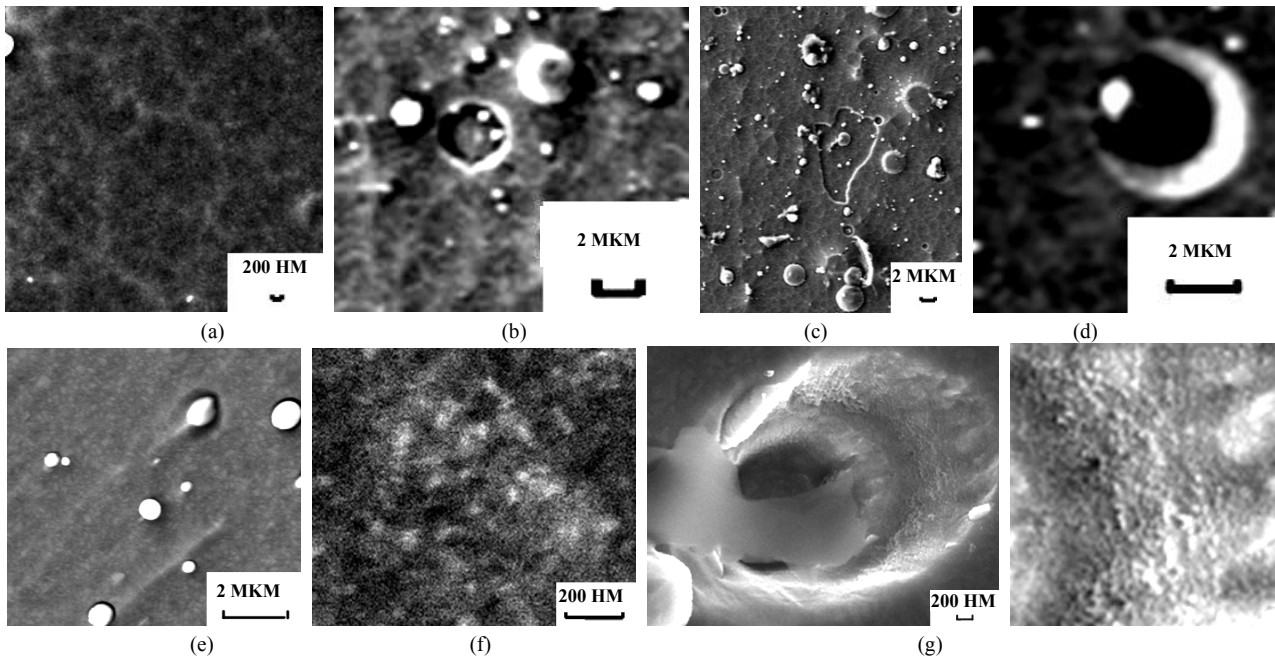


**Figure 8.** Photomicrographs of TiN film on stage of continuous film forming: with cellular structure (a) Cell  $\text{\O}$  900 nm to 3.0  $\mu\text{m}$  at 50% of nitrogen, and (c) Cells  $\text{\O}$  700 nm to 2.0  $\mu\text{m}$  at 70%; with grain substructure (e), (f) Light grains of 30 nm, dark grains of 50 nm, both at 90% of nitrogen. Film material “lack”: (b) 2.5  $\mu\text{m}$  at 50%; (c) 8.5  $\mu\text{m} \times 15.0 \mu\text{m}$ , (d) 3.5  $\mu\text{m}$ , both at 70%; (g) 90%, 3.4  $\mu\text{m}$ , forced fragment to the right shows that minimum size of crystallite does not exceed 20 nm.

The material “lack” of the ionic plasma film increases along with increasing of the nitrogen concentration in the mixed gas (**Figures 8(b-d, g)**). Minimum size of the film uniformity, nano-crystalline structure of a chip, minimum size of seed crystallite, fine grain substructure of the film are indicative for the following forming conditions: 90% of nitrogen,  $T = 645 \dots 725 \text{ K}$ ,  $V_{\text{film heat}} = 14.2 \text{ K/min}$  (**Figures 8(e-g)**).

Stage of forming of ordered 2D and 3D formations on the continuous film surface. Independently on technological and temperature conditions of the film forming, microscopic formations are forming on film’s surface after 30 minutes as a result of integration of 2D and 3D formations (**Figure 9**). At 70% nitrogen concentration, solitary 3D formations with ordered grain substructure appear on the continuous film surface (**Figure 9(a)**) which worsen film surface quality (were not observed in earlier experiments). At maximum nitrogen concentration of 90% we can observe on film surface 2D rod-shaped formations having ordered column substructure (**Figure 9(b)**).

#### 4. Summary

A phase-structural condition of the TiN films formed by arc spraying at various nitrogen concentrations has been investigated by method of X-ray diffraction phase analysis. It was first established that decreasing of the nitrogen concentration less than 70% leads to increasing of vol-

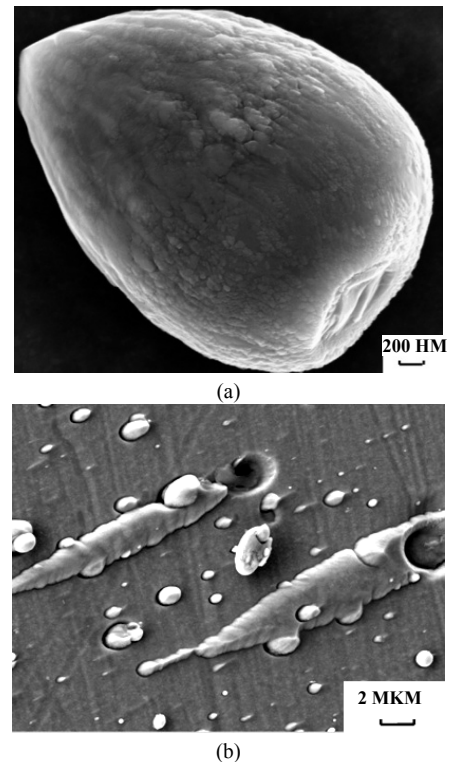


**Figure 9.** Photomicrographs of the TiN on stage of the continuous film forming with surface structures in form of: (a) 3D formations sized as  $3.0 \times 4.2 \times 1.2 \mu\text{m}$  at 70%, and (b) 2D rod-shaped formations with length of 20  $\mu\text{m}$  and width of 3  $\mu\text{m}$  at 90%.

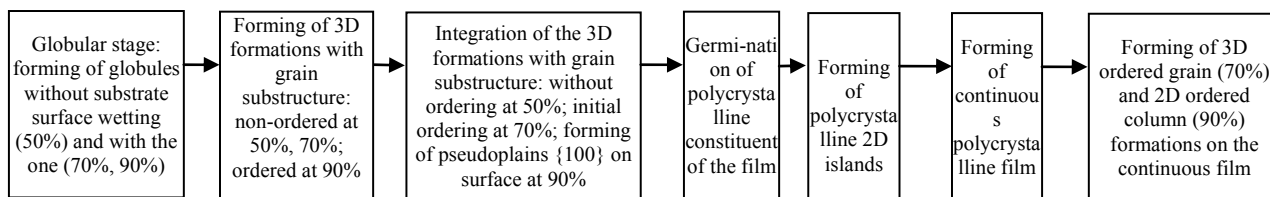


**Figure 10.** Stages of the TiN film forming depending on nitrogen concentration in mixed gas, film temperature, and film heating rate. Forming of films with main cubic TiN phase by arc spraying method (50% of N<sub>2</sub>, 625 to 670 K, V<sub>film heating</sub> = 12.3 K/min; 70% of N<sub>2</sub>, 625 to 680 K, V<sub>film heating</sub> = 12.5 K/min; 90% of N<sub>2</sub>, 645 to 725 K, V<sub>film heating</sub> = 14.2 K/min).

ume fraction of the hexagonal TiN<sub>0.3</sub> phase and to worsening of its mechanical properties.

Structuring of the films with main cubic (111) TiN phase goes through the following stages: globular, forming of 3D formations with grain substructure, integration of the 3D formations, nucleation of polycrystalline constituent of the film, forming of polycrystalline 2D islands, forming of continuous film, forming of ordered 3D and 2D formations on the continuous film surface (**Figure 10**).

In summary, it was discovered that except of film temperature film heating rate first of all effect on origin, forming stages, and structuring of the ion-plasma TiN films in process of the film applying.

## REFERENCES

- [1] A. F. Belyanin and M. I. Samoylovich, "Diamond and Diamond-Like Materials Films: Formation, Structure and Applications in Electronics," (In Russia), CRTI Technomash, Moscow, 2004.
- [2] P. H. Mayrhofer, F. Kunc, J. Musil and C. Mitterer, "A Comparative Study on Reactive and Non-Reactive Unbalanced Magnetron Sputter Deposition of TiN Coatings," *Thin Solid Films*, Vol. 415, No. 1-2, 2002, pp. 151-159. [doi:10.1016/S0040-6090\(02\)00511-4](https://doi.org/10.1016/S0040-6090(02)00511-4)
- [3] J. Musil, "Hard and Superhard Nanocomposite Coatings," *Surface and Coatings Technology*, Vol. 125, No. 1-3, 2000, pp. 322-330. [doi:10.1016/S0257-8972\(99\)00586-1](https://doi.org/10.1016/S0257-8972(99)00586-1)
- [4] I. Petrov, P. B. Varna, L. Hultman and J. E. Greene, "Microstructural Evolution during Film Growth," *Journal of Vacuum Science and Technology A*, Vol. 21, No. 5, 2003, pp. 117-128. [doi:10.1116/1.1601610](https://doi.org/10.1116/1.1601610)
- [5] J. Thornton, "High-Rate Thick-Film Growth," *Annual Review of Materials Science*, Vol. 7, 1977, pp. 239-260. [doi:10.1146/annurev.ms.07.080177.001323](https://doi.org/10.1146/annurev.ms.07.080177.001323)
- [6] R. Messier, A. P. Giri and R. A. Roy, "Revised Structure Zone Model for Thin Film Physical Structure," *Journal of Vacuum Science and Technology A*, Vol. 2, 1984, pp. 500-503. [doi:10.1116/1.572604](https://doi.org/10.1116/1.572604)
- [7] J. A. Thornton, "The Microstructure of Sputter-Deposited Coatings," *Journal of Vacuum Science and Technology A*, Vol. 4, No. 6, 1986, pp. 3059-3056. [doi:10.1116/1.573628](https://doi.org/10.1116/1.573628)
- [8] P. B. Barna and M. Adamik, "Fundamental Structure Forming Phenomena of Polycrystalline Films and the Structure Zone Models," *Thin Solid Films*, Vol. 317, 1998, pp. 27-33. [doi:10.1016/S0040-6090\(97\)00503-8](https://doi.org/10.1016/S0040-6090(97)00503-8)
- [9] S. Kadlec, J. Musil and J. Vyskočil, "Growth and Properties of Hard Coating Prepared by Physical Vapor Deposition Methods," *Surface and Coatings Technology*, Vol. 54-55, 1992, pp. 287-296.
- [10] L. I. Maissel, "Handbook of Thin Films," McGraw-Hill, New York, 1983.
- [11] R. Messier, "Toward Quantification of Thin Film Morphology," *Journal of Vacuum Science and Technology A*, Vol. 4, No. 3, 1986, pp. 490-495. [doi:10.1116/1.573866](https://doi.org/10.1116/1.573866)
- [12] M. Stüber, H. Leiste, S. Ulrich, H. Holleck and D. Schild, "Microstructure and Properties of Low Friction Ti-C Nanocomposite Coatings Deposited by Magnetron Sputtering," *Surface and Coatings Technology*, Vol. 150, No. 2-3, 2002, pp. 218-226. [doi:10.1016/S0257-8972\(01\)01493-1](https://doi.org/10.1016/S0257-8972(01)01493-1)
- [13] V. N. Antsiferov and A. L. Kameneva, "Experimental Study of the Structure of Multicomponent Nanostructured Coatings on the Basis of Ti-Zr-N Alloys Formed by Ionic Plasma Methods," *Russian Journal of Non-Ferrous Metals*, Vol. 48, No. 6, 2007, pp. 488-495. [doi:10.3103/S1067821207060211](https://doi.org/10.3103/S1067821207060211)
- [14] D. V. Shtansky, E. A. Levashov, K. Kaneko and Y. Ikuhara, "Characterization of Nanostructured Multiphase Ti-Al-B-N Thin Films with Extremely Small Grain Size," *Surface and Coatings Technology*, Vol. 148, No. 2-3, 2001, pp. 206-215. [doi:10.1016/S0257-8972\(01\)01341-X](https://doi.org/10.1016/S0257-8972(01)01341-X)
- [15] D. V. Shtansky, E. A. Levashov, A. N. Sheveiko and J. J. Moore, "Synthesis and Characterization of Ti-Si-C-N Films," *Metallurgical and Materials Transaction A*, Vol. 30, No. 9, 1999, pp. 2439-2447. [doi:10.1007/s11661-999-0252-0](https://doi.org/10.1007/s11661-999-0252-0)
- [16] A. Gupper, A. Fernandez, C. Fernandez-Ramos, F. Hofer, C. Mitterer and P. Warbichler, "Characterization of Nanocomposite Coatings in the System Ti-B-N by Analytical Electron Microscopy and X-Ray Photoelectron Spectroscopy," *Monatshefte für Chemie/Chemical Monthly*, Vol. 133, No. 6, 2002, pp. 837-848.

- [17] T. P. Mollart, P. N. Gibson and M. A. Baker, "An EXAFS and XRD Study of the Structure of Nanocrystalline Ti-B-N Thin Films," *Journal of Physics D: Applied Physics*, Vol. 30, No. 13, 1997, pp. 1827-1832.  
[doi:10.1088/0022-3727/30/13/001](https://doi.org/10.1088/0022-3727/30/13/001)
- [18] W. Gissler. "Structure and Properties of Ti-B-N Coatings," *Surface and Coatings Technology*, Vol. 68-69, 1994, pp. 556-563.
- [19] J. Musil, F. Kunc, H. Zeman and H. Polakova, "Relationships between Hardness, Young's Modulus and Elastic Recovery in Hard Nanocomposite Coatings," *Surface and Coatings Technology*, Vol. 154, No. 2-3, 2002, pp. 304-313.  
[doi:10.1016/S0257-8972\(01\)01714-5](https://doi.org/10.1016/S0257-8972(01)01714-5)